Optical signatures of type I - type II band alignment transition in Cd(Se,Te)/ZnTe self-assembled quantum dots

Piotr Baranowski[1], Małgorzata Szymura[1], Grzegorz Karczewski[1], M. Aleszkiewicz[1], Aleksander Rodek[3], Tomasz Kazimierczuk[3], Piotr Kossacki[3], Tomasz Wojtowicz[1,2], Jacek Kossut[1], Piotr Wojnar[1a)]

1. Institute of Physics, Polish Academy of Sciences, Al Lotników 32/46, PL-02-668 Warsaw, Poland
2. *International Research Centre MagTop, Institute of Physics, Polish Academy of Sciences, Al Lotników 32/46, PL-02-668 Warsaw, Poland*
3. Institute of Experimental Physics, Faculty of Physics, University of Warsaw, ul Pasteura 5, PL-02-093 Warsaw, Poland

Abstract

Self-assembled Cd(Se,Te) quantum dots with various Se compositions embedded in ZnTe matrix are grown by molecular beam epitaxy. A huge redshift of the near band edge emission, from 2.1 eV to 1.5 eV, with an increasing Se content in the dots is observed. It is accompanied by an increase of the excitonic lifetime by the factor of 10. We associate these effects to a gradual change from the direct type I confinement character in CdTe/ZnTe quantum dots to the staggered type II band alignment in the case of Cd(Se,Te)/ZnTe dots. This interpretation is consistent with the micro-photoluminescence study of several individual quantum dots, which reveals a gradual decrease of the biexciton-exciton energy difference with increasing content of Se in the dots which leads ultimately to the change from binding to antibinding character of biexcitons. The latter effect originates, most likely, from the increasing Coulomb repulsion between excitons forming dipoles at the dot/barrier interface.

Semiconductor heterostructures can be classified either as type I or type II depending on the relative alignment of conduction and valence band edges. In type I heterostructures electrons and holes are localized in the semiconductor with the smaller energy gap. On the other hand, the type II heterostructures are characterized by a staggered band alignment, which leads to the spatial separation of electrons and holes at the interface, as shown in Figure 1a. Quantum dots (QDs) with a staggered type II band alignment between the dot and barrier semiconductors exhibit several important advantages compared to their thoroughly-studied type I counterparts. First of all, their optical emission can be tuned in a quite broad spectral range due to variation of band edge energies. In particular, one may access the spectral range which is not covered by the energy gaps of semiconductors constituting heterojunctions[1–3]. This property has enabled, for instance, the applications of wide band gap semiconductors, such as ZnO/ZnSe, in photovoltaic devices[4–6]. Another important advantage resulting directly from the electron-hole spatial separation is the suppression of non-radiative Auger recombination in type II core/shell QDs[7–9]. Thanks to this effect, the optical gain has been observed even in the low excitation single-exciton

a) Corresponding author, email: wojnar@ifpan.edu.pl

regime[7], opening a path toward the applications of type II QDs in the field of lasing technologies. This result is particularly interesting in the context of a recent report about the fabrication of high performance light emitting diodes[10] based on Se-containing type I core/shell QDs. On the other hand, the quite small overlap of electron and hole wavefunctions typical for type II heterostructures results in the reduction of the optical emission intensity and in long decays. Therefore, controlling the latter effect might be crucial in view of potential application in lightening devices.

In most reports concerning optical properties of type II QDs, either ensembles of colloidal core/shell nanocrystals[1,2,11] or ensembles of self-assembled QDs built of III-V[12–14] or II-VI[15,16] semiconductors grown by epitaxial methods were investigated. There is only a limited number of publications about the emission from single type II nanostructures[9,17,18]. They concern, for instance, the optical stability and blinking behavior of type II QDs[9], as well as a bicolor emission from single type II core/crown nanoplatelet heterostructures[17]. Multiexcitonic complexes from a single dot have been observed only in the case of Cd(Se,Te)/ZnSe QDs[18] in which a rather small carrier separation effect originates from alloy fluctuations inside the dots. Preforming single dot spectroscopy on a single type II QD could be advantageous in the context of a recent publication predicting a significant reduction of the excitonic fine structure splitting in the emission spectra [19] which could lead to the creation of polarization entangled photon pairs. Moreover, the electron-hole spatial separation in type II ZnTe/ZnSe QDs columns results in the presence of coherently rotating states leading to the observation of Aharonov-Bohm oscillations in an external magnetic field[20,21].

In this work, we demonstrate a well-controlled transition from type I to type II character of the band alignment in Cd(Se,Te)/ZnTe QDs resulting from the increase of Se-concentration inside the dots. This transition is accompanied by a huge redshift of the emission energy of about 600 meV and an increase of the excitonic lifetime by one order of magnitude resulting directly from the electron-hole separation effect. Moreover, optical emission spectra from individual dots reveal the presence of several multiexcitonic complexes. In particular, a gradual change from binding to antibinding character of biexcitons with an increasing Se concentration is found to be an additional important signature of the type I to type II confinement transition in QDs.

Self-assembled Cd(Se,Te)/ZnTe quantum dots (QDs) are grown in the molecular beam epitaxy (MBE) system consisting of two growth chambers connected to each other through ultra-high vacuum transfer chamber. The first growth chamber (EPI 620) is dedicated to the growth of tellurium based semiconductors and contains Cd, Zn and Te effusion cells, whereas the second chamber (from PREVAC) is equipped with Cd and Se effusion cells. All atomic fluxes are characterized by the beam equivalent pressure (BEP) being of the order of 10^{-7} torr. The samples are grown on a 4 µm thick CdTe buffer deposited on (100)-oriented GaAs substrate in a separate process. After thermal treatment of CdTe/GaAs hybrid substrate the growth starts with a 1.5 µm thick ZnTe barrier layer deposited at 320°C. It is followed directly by the QDs-layer which

consists of six monolayers, 2 CdTe full monolayers, 1 CdSe (submonolayer) and 3 CdTe monolayers. The highest average Se concentration within the dots can be, therefore, estimated to 16.7%. One has to note, however, that in these considerations we neglect the effect of isovalent substitution of Te atoms with Se, which may lead to the underestimation of this value.

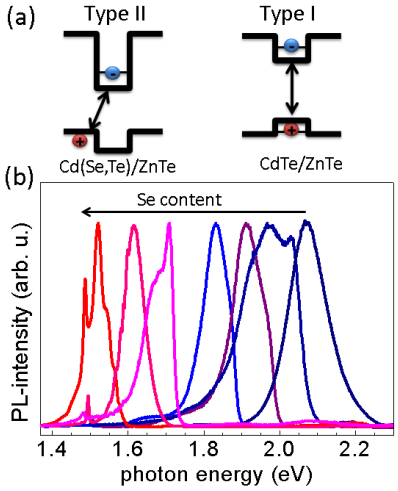

Figure 1 (a) Band edge alignment in type II (left) and type I (right) heterostructures; arrow – optical transition (b) Photoluminescence from Cd(Se,Te)/ZnTe self-assembled quantum dots with various Se concentrations. The spectrum with the maximum at 2.1 eV comes from pure CdTe/ZnTe quantum dots. A considerable emission redshift is observed with increasing Se content inside the dots. The QDs were excited by 473 nm laser line at 6 K.

Depending on a particular sample the coverage of the central CdSe – layer is governed by Se-deposition time. To be more precise, the QDs layer starts with two CdTe monolayers grown by alternating opening Cd and Te fluxes for 8 seconds at 280°C in the first growth chamber. Next, the sample is moved to the second growth chamber through the ultra-high vacuum transfer chamber for CdSe deposition. The substrate temperature in the second growth chamber is raised up to 280°C and stabilized under Cd flux for 20 minutes. Then, Cd-flux is switched off and Se-flux opened for a certain time period ranging from 10 s to 60 s depending on a particular sample. Subsequently, the substrate temperature is decreased under Cd flux and the sample is moved back to the first chamber. The substrate temperature of 280°C is stabilized again under Cd flux for 30 minutes and the consecutive 3 CdTe monolayers are deposited by the alternating opening of Cd and Te fluxes for 8 seconds. The QDs formation process is induced by the Te covering method, i.e., by covering the surface with crystalline Te layer at low substrate temperature and its thermal desorption[22,23]. This process is monitored by the Reflection High Energy Electron Diffraction

(RHEED) which shows a distinct change from two dimensional to three dimensional character of the surface typical for the formation of self-assembled QDs, which appears independently of the coverage of the central CdSe-layer (Supplementary Material, Figure S1). The final step consists of the deposition of a 60 nm thick ZnTe cap layer at 320°C.

Interestingly, when introducing more than one CdSe monolayer into 6 monolayers thick CdTe/CdSe/CdTe layer the QDs-formation process does not take place. This is manifested by an absence of the characteristic 2D-3D transition of the RHEED pattern (Supplementary Material) and confirmed by the absence of single dot emission in microphotoluminescence spectra, as discussed further in the text. The interpretation of this observation involves the reduction of the lattice mismatch between the dot and barrier semiconductors which is the driving force inducing the QDs formation process.

At this stage, it should be noted that the use of CdTe/CdSe/CdTe multilayer as a starting point for the formation of QDs reduces also the probability of the creation of ZnSe interfacial layers which has been observed at CdSe/ZnTe interfaces[24].

Low temperature photoluminescence (PL) spectra are measured for all Cd(Se,Te)/ZnTe QDs with various Se concentrations. For these measurements, the samples are placed in a closed cycle helium cryostat at 6 K, and are excited with a 473 nm solid state laser. The signal is detected in a 303 mm monochromator (SR303i by Andor) equipped with a CCD camera. The results of these measurements are presented in Figure 1b. Most importantly, a huge emission energy redshift from 2.1 eV to 1.5 eV is observed as a result of increasing Se-concentration inside the dots. Moreover, we demonstrate that the emission energy can be tuned continuously to any energy within this spectral range by the variation of CdSe layer coverage controlled during the growth process.

The interpretation of this result relies on a transition from type I to type II band alignment induced by an increasing incorporation of Se into Cd(Se,Te) QDs embedded in ZnTe matrix. As already well established, self-assembled CdTe/ZnTe QDs are characterized by type I confinement which is manifested by relatively short exciton lifetimes of the order of hundreds of picoseconds[25]. On the other hand, the valence band offset in this common anion semiconductor system is quite small and is mostly caused by the strain and excitonic effects[26]. This results, for instance, in an efficient thermal escape of holes at elevated temperatures leading to thermally induced quenching of the PL-intensity[27,28]. Introduction of Se atoms into CdTe dots shifts both, valence and conduction band edges, toward lower energies which leads to a transition from type I to type II character of the confinement[29], Figure 1a. Electrons are confined inside the dots and holes are pushed outside of them. The larger Se concentration the larger electron-hole wavefunction separation takes place. The extreme case of CdSe/ZnTe semiconductor system is well-known for its type II staggered band alignment with the optical transition energy at 1.01 eV,

i.e., well below the energy gaps of ZnTe and CdSe[30]. However, self-assembled QDs cannot be formed in this semiconductor system due to the small lattice mismatch.

At this stage, it should be discussed whether additional effects, such as QDs size variation and strain conditions within the dots, could also contribute to the observed giant emission energy shift. Atomic Force Miscroscope (AFM) studies performed on uncapped dots reveal that the presence of Se inside the dots in concentrations typical for this study does not affect significantly the QDs morphology (see Supplementary Material, Figure S2). Moreover, we find also that the increase of the QDs layer thickness from five to eight monolayers in the case of pure CdTe/ZnTe QDs does not change importantly the emission energy which appears always in the 2.1 eV - 2.2 eV spectral range. These two results indicate that the QDs size variation does not contribute significantly to the observed redshift of the optical emission. On the other hand, the introduction of Se into Cd(Se,Te)/ZnTe QDs leads to the decrease of the lattice mismatch between the dot and the barrier semiconductor. The reduction of the strain within the dots is an important effect which may contribute significantly to the emission energy in addition to the variation of band edge energies. Finally, we find that the emission from the Cd(Se,Te)/ZnTe QDs with the highest Se concentrations appears at energies lower than the bandgaps of CdTe (1.59 eV), CdSe (1.74 eV) and ZnTe (2.39 eV), Figure 1b. The latter effect can be explained only by the type II staggered band alignment.

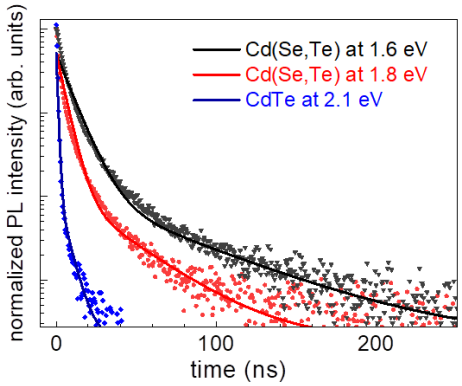

Figure 2 Normalized time-resolved PL decays from CdTe/ZnTe and Cd(Se,Te)/ZnTe QDs with a moderate and high Se concentration emitting at 2.1 eV, 1.8 eV and 1.6 eV, respectively. The temperature of the measurement is 7 K and the excitation wavelength 400 nm; solid lines are fits with biexponential functions (see text).

The type II confinement in Cd(Se,Te)/ZnTe QDs is directly evidenced based on the study of PL-decays from the structures with various Se concentrations. A significant increase of the excitonic

lifetime is expected in QDs with the staggered type II band alignment due to decreasing electron-hole overlap as compared to their type I counterparts. This is, in fact, what is observed in our experiment. For time resolved PL (TRPL) measurements, the samples are excited by picosecond laser pulses at 400 nm wavelength. The temporal pulse width of 128 ps for 5 MHz repetition rate is used for TRPL measurements of bare CdTe/ZnTe QDs, whereas the temporal pulse width of 512 ps for 2 MHz repetition rate is used for Cd(Se,Te)/ZnTe QDs, where significantly longer decays are observed. The signal is detected with a single-photon counting avalanche photodiode.

In Figure 2, normalized TRPL traces from bare CdTe and Cd(Se,Te) QDs with two different Se concentrations: moderate emitting at 1.8 eV and relatively high emitting at 1.6 eV, are presented. We observe that the decay times strongly depend on Se concentration inside the dots. The decay time from pure CdTe/ZnTe QDs is almost at the limit of the temporal resolution of our setup whereas it increases conspicuously for moderate and, even more, for high Se concentrations inside of the dots. PL-transients for all studied samples are highly non-exponential and can be fitted by biexponential decays. Different decay mechanisms are related, most likely, to the presence of emission lines from single excitons and multiexcitonic complexes within the type II QD ensemble. Following this interpretation, the long decay time corresponds to the recombination of single excitons and amounts to 5.6 ns, 32 ns and 57 ns for CdTe and Cd(Se,Te) QDs with moderate and high Se concentration, respectively. On the other hand, the fast component of the PL-decays is associated to multiexcitonic complexes, which are characterized typically by a relatively large number of decay channels[31,32]. In the case of type II heterostructures, however, the multiexcitonic decay time may be additionally reduced due the band bending resulting from the electron-hole pair accumulation at the interfaces[30,33]. The short decay times are found to be 0.8 ns, 4.9 ns and 8 ns in CdTe and Cd(Se,Te) QDs with moderate and high Se concentration, respectively. Most importantly, we realize that the long and short decay times increase both by the factor of about 10 as result of increasing Se concentration inside Cd(Se,Te) QDs. The gradual increase of the PL lifetime with increasing Se content results directly from carrier separation at the interface and strongly supports our interpretation in terms of a type I to type II confinement transition in Cd(Se,Te)/ZnTe QDs.

In order to investigate the emission from individual QDs, a standard setup for micro-photoluminescence (μ-PL) is used. The laser beam with the wavelength of 473 nm is focused onto ~3 μm spot with a microscope objective, whereas the emitted light is collected by the same objective and detected by a 500 mm-monochromator (SR-500i by Andor) equipped with a CCD camera. For these measurements, the sample is placed again on a cold finger cryostat at 7 K. In order to reduce the number of QDs excited simultaneously with the laser beam, 100 nm thick gold layer with 300 nm - diameter apertures is deposited on the top of the samples[34].

First of all, we observe that the quite broad emissions from Cd(Se,Te)/ZnTe QDs split into several sharp lines with the spectral width of the order of a few meV originating from individual QDs. This effect takes place in all studied samples emitting in the spectral range from 2.1 eV to

1.5 eV independently on the Se concentration inside of them. At this stage, it should be noted that in the case of Cd(Se,Te)/ZnTe heterostructures where more than one CdSe monolayer is introduced into the 6 monolayers thick CdTe/CdSe layer, emission lines from individual QDs cannot be resolved, even in the samples with apertures. Therefore, we conclude that the QDs formation process has not taken place in these heterostructures and that they should be regarded as type II Cd(Se,Te)/ZnTe quantum wells. These samples are out of the scope of this report.

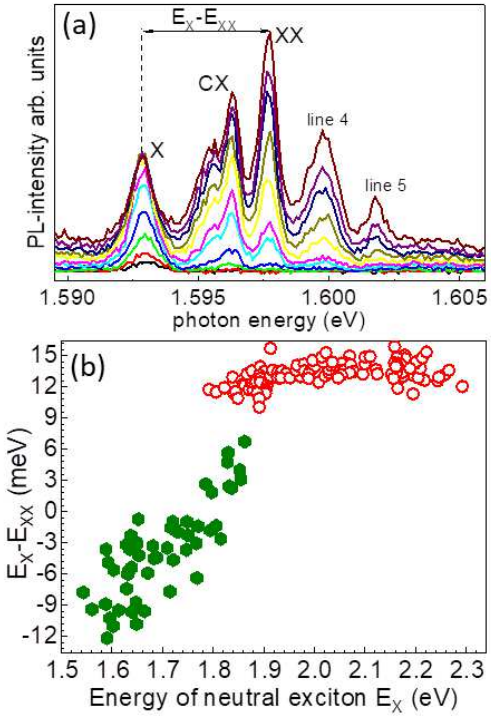

Figure 3 a) Optical emission spectrum from an individual Cd(Se,Te)/ZnTe quantum dot at various excitation powers ranging from 300 μW to 30 mW. The lines are ascribed either to single exciton – X, charged exciton - CX and biexciton - XX emission (see text) b) The biexciton binding energy defined as X - XX spectral distance versus the X emission energy plotted for several individual quantum dots revealing a gradual change from binding to antibinding character of biexcitons. Green points - Cd(Se,Te) QDs from several samples with various Se concentrations, red circles – pure CdTe QDs, reproduced with permission from Physical Review B 84, 165319 (2011), copyright 2011 American Physical Society[35]. The temperature of the measurement is always 7 K, and the excitation performed with 473 nm laser line.

In Figure 3a, a typical excitation fluence dependence of the emission spectrum from a single Cd(Se,Te) QD is presented. This particular dot originates from the sample characterized by PL-maximum at 1.6 eV. In the low excitation regime, the optical emission spectrum consists of only one emission line at 1.593eV (Supplementary Material, S3). With an increasing excitation fluence additional PL-lines appear consecutively at higher energies. The PL-intensity dependence on the excitation fluence for all these lines are presented in the Supplementary Material, Figure S3. The intensity of the peak at 1.593 eV increases almost linearly and saturates at relatively high fluences, which is a typical behavior of the single exciton line, X. On the other hand, the emission intensity of the line at 1.598 eV increases superlinearly with the exponent 2.0 which leads us to associate it with biexciton emission, XX. The double peak at 1.596 eV, i.e., spectrally between X and XX, is, most likely, related to singly charged excitons, CX. The emission intensities of PL-lines appearing at relatively high energies, i.e., at 1.600 eV and 1.602 eV, increase quite fast with the excitation fluence and are characterized by exponents equal to 2.1 and 2.5, respectively. They can be associated, therefore, to multiexcitonic complexes involving even more charge carriers such as charged biexcitons or triexcitons. It should be noted here, that the long carrier lifetimes in type II heterostructures may facilitate the formation of multiexcitonic complexes in type II QDs. Similar spectra are recorded for several individual QDs. In many cases, however, the emission spectrum consists of X and XX emission lines only. CX line cannot be identified. Another example of a single dot emission from a Cd(Se,Te) QD with a relatively small Se concentration is demonstrated in the Supplementary Material, Figure S4.

Most importantly, multiexcitons in type II Cd(Se,Te)/ZnTe QDs appear always at *higher* energies than single excitons. This finding is, in fact, opposite to the effect observed previously for type I CdTe/ZnTe QDs[35]. In the case of the latter, multiexcitonic complexes have been found to be always characterized by a *lower* energy compared to single excitons. In order to assess this effect in a detailed manner, a systematic study of the emission from several individual Cd(Se,Te)/ZnTe QDs with various Se concentrations from several samples emitting in the spectral range from 1.5 eV up to 1.9 eV has been performed. In particular, we focus on the biexciton binding energy defined as X-XX energy difference. We find that this quantity depends strongly on Se-concentration in the dots, Figure 3b. In the case of pure CdTe/ZnTe QDs the biexciton binding energy is always positive revealing a binding character of biexcitons. Its value is quite similar for all dots, in the range from 12 meV to 15 meV[35]. After introduction of Se into the dots, a gradual reduction of the biexciton binding energy takes place leading finally to the change of the sign for the dots emitting at energies below 1.7 eV. We attribute this effect to the increasing electron - hole spatial separation at the type II interface which leads to the gradual increase of repulsive Coulomb interaction between the single-sign charge carriers in the biexciton complex. As an effect, a change from binding to antibinding character of biexcitons occurs.

At this stage, it should be noted that similar transition from binding to antibinding biexciton character has already been observed in GaN/AlN QDs[36]. In this completely different semiconductor system, size dependent charge carrier separation takes place on the basis of large

spontaneous and piezoelectric polarization and not due to the type II band alignment. On the other hand, a strong antibinding of biexcitons has been theoretically predicted in type II core/shell colloidal nanocrystals[37]. Therefore, we conclude that the experimental observation of a gradual transition from binding to antibinding character of biexcitons is a further important signature of the type I to type II confinement transition.

The appearance of multiexcitonic complexes at higher energies than the single exciton emission is, in fact, an analogous effect to that observed previously in type II quantum wells. In those heterostructures a prominent blueshift of the emission energy with increasing excitation fluence has been observed which is presently regarded as the hallmark of the type II confinement[30,38]. The mechanism laying behind this effect can be summarized as follows: an increasing excitation fluence results in the charge carriers accumulation at interfaces and formation of electric dipoles. The resulting electric field is proportional to the number of charge carriers and leads to an effective increase of the emission energy. In contrast to quantum wells, however, the number of electrons and holes confined inside a QD is limited. Therefore, only a discrete number the emission lines appears at higher energies than the excitonic line. Although the emission energy of the lines associated to individual multiexcitonic complexes stay almost unchanged with an increasing excitation fluence, the overall center of the luminescence from a single QD shows a blueshift similar to type II quantum wells.

In summary, Cd(Se,Te)/ZnTe QDs with various Se concentrations controlled by the Se deposition time are grown in a MBE process. We find that the properties of the optical emission from these structures are strongly affected by the composition of the dots. First of all, a huge redshift of the emission energy of about 600 meV, from 2.1 eV to 1.5 eV is observed as result of increasing Se-concentration. Secondly, we find that the PL decay time increases simultaneously by one order of magnitude. Finally, the study of several individual QDs emission reveals that the biexciton binding energy (X-XX spectral distance) changes gradually its character from binding to antibinding with an increasing Se concentration. All these effects can be explained in terms of a transition from type I to type II confinement. The redshift of the emission results from the variation of conduction and valence band in Cd(Se,Te) as a function of Se concentration. The increase of the PL-decay times reflects directly the spatial separation of electron - hole wavefunctions. Finally, the variation of the biexciton binding energy is caused by the increase the repulsive exciton-exciton Coulomb interaction due to electron-hole separation at the type II interface. The latter effect represents, therefore, an additional important signature of the type I to type II confinement type transition in quantum dots.

Supplementary material

See supplementary material for RHEED pattern, AFM study of Cd(Se,Te) QDs, and micro-photoluminescence (μ-PL) from a QD with a relatively small Se concentration.

Acknowledgements

This work has been partially supported by the National Centre of Science (Poland) through grant 2017/26/E/ST3/00253, and by the Foundation for Polish Science through the IRA Programme co-financed by the EU within SG OP. AR, TK and PK acknowledge support by the ATOMOPTO project carried out within the TEAM programme of the Foundation for Polish Science co-financed by the EU under the ERD-Fund.

Data Statement

The data that support the findings of this study are available from the corresponding author upon reasonable request

References

[1] S.A. Ivanov, A. Piryatinski, J. Nanda, S. Tretiak, K.R. Zavadil, W.O. Wallace, D. Werder, and V.I. Klimov, J. Am. Chem. Soc. **129**, 11708 (2007).

[2] S. Kim, B. Fisher, H.J. Eisler, and M. Bawendi, J. Am. Chem. Soc. **125**, 11466 (2003).

[3] V. Deligiannakis, S. Dhomkar, M.S. Claro, I.L. Kuskovsky, and M.C. Tamargo, J. Cryst. Growth **512**, 203 (2019).

[4] Y. Zhang, Z. Wu, J. Zheng, X. Lin, H. Zhan, S. Li, J. Kang, J. Bleuse, and H. Mariette, Sol. Energy Mater. Sol. Cells **102**, 15 (2012).

[5] Q. Yang, H. Cai, Z. Hu, Z. Duan, Y. Li, J. Sun, N. Xu, and J. Wu, Mater. Res. Express **1**, 015010 (2014).

[6] X. Yang, Q. Yang, Z. Hu, W. Zhang, H. Li, L. Li, Y. Qiu, N. Xu, J. Wu, and J. Sun, RSC Adv. **6**, 98413 (2016).

[7] V.I. Klimov, S.A. Ivanov, J. Nanda, M. Achermann, I. Bezel, J.A. McGuire, and A. Piryatinski, Nature **447**, 441 (2007).

[8] Y. Gao, M. Li, S. Delikanli, H. Zheng, B. Liu, C. Dang, T.C. Sum, and H.V. Demir, Nanoscale **10**, 9466 (2018).

[9] A.M. Dennis, B.D. Mangum, A. Piryatinski, Y.S. Park, D.C. Hannah, J.L. Casson, D.J. Williams, R.D. Schaller, H. Htoon, and J.A. Hollingsworth, Nano Lett. **12**, 5545 (2012).

[10] H. Shen, Q. Gao, Y. Zhang, Y. Lin, Q. Lin, Z. Li, L. Chen, Z. Zeng, X. Li, Y. Jia, S. Wang, Z. Du, L.S. Li, and Z. Zhang, Nat. Photonics **13**, 192 (2019).

[11] H. Eshet, M. Grünwald, and E. Rabani, Nano Lett. **13**, 5880 (2013).

[12] W.T. Hsu, Y.A. Liao, F.C. Hsu, P.C. Chiu, J.I. Chyi, and W.H. Chang, Appl. Phys. Lett. **99**, 073108 (2011).

[13] Y.I. Mazur, V.G. Dorogan, G.J. Salamo, G.G. Tarasov, B.L. Liang, C.J. Reyner, K. Nunna, and D.L. Huffaker, Appl. Phys. Lett. **100**, 033102 (2012).

[14] Y.D. Jang, T.J. Badcock, D.J. Mowbray, M.S. Skolnick, J. Park, D. Lee, H.Y. Liu, M.J. Steer,

and M. Hopkinson, Appl. Phys. Lett. **92**, 251905 (2008).

[15] H. Ji, S. Dhomkar, R. Wu, V. Shuvayev, V. Deligiannakis, M.C. Tamargo, J. Ludwig, Z. Lu, D. Smirnov, A. Wang, and I.L. Kuskovsky, J. Appl. Phys. **119**, 224306 (2016).

[16] M.C. Kuo, J.S. Hsu, J.L. Shen, K.C. Chiu, W.C. Fan, Y.C. Lin, C.H. Chia, W.C. Chou, M. Yasar, R. Mallory, A. Petrou, and H. Luo, Appl. Phys. Lett. **89**, 263111 (2006).

[17] M. Dufour, V. Steinmetz, E. Izquierdo, T. Pons, N. Lequeux, E. Lhuillier, L. Legrand, M. Chamarro, T. Barisien, and S. Ithurria, J. Phys. Chem. C **121**, 24816 (2017).

[18] M. Ściesiek, J. Suffczyński, W. Pacuski, M. Parlińska-Wojtan, T. Smoleński, P. Kossacki, and A. Golnik, Phys. Rev. B **93**, 195313 (2016).

[19] V. Křápek, P. Klenovský, and T. Šikola, Phys. Rev. B - Condens. Matter Mater. Phys. **92**, 195430 (2015).

[20] I.R. Sellers, V.R. Whiteside, I.L. Kuskovsky, A.O. Govorov, and B.D. McCombe, Phys. Rev. Lett. **100**, 136405 (2008).

[21] I.L. Kuskovsky, L.G. Mourokh, B. Roy, H. Ji, S. Dhomkar, J. Ludwig, D. Smirnov, and M.C. Tamargo, Phys. Rev. B **95**, 165445 (2017).

[22] F. Tinjod, B. Gilles, S. Moehl, K. Kheng, and H. Mariette, Appl. Phys. Lett. **82**, 4340 (2003).

[23] P. Wojnar, C. Bougerol, E. Bellet-Amalric, L. Besombes, H. Mariette, and H. Boukari, J. Cryst. Growth **335**, 28 (2011).

[24] B. Bonef, L. Gérard, J.L. Rouvière, A. Grenier, P.H. Jouneau, E. Bellet-Amalric, H. Mariette, R. André, and C. Bougerol, Appl. Phys. Lett. **106**, 051904 (2015).

[25] T. Kazimierczuk, M. Goryca, M. Koperski, A. Golnik, J.A. Gaj, M. Nawrocki, P. Wojnar, and P. Kossacki, Phys. Rev. B - Condens. Matter Mater. Phys. **81**, 155313 (2010).

[26] E. Deleporte, J.M. Berroir, C. Delalande, N. Magnea, H. Mariette, J. Allegre, and J. Calatayud, Phys. Rev. B **45**, 6305 (1992).

[27] F. Tinjod, S. Moehl, K. Kheng, B. Gilles, and H. Mariette, J. Appl. Phys. **95**, 102 (2004).

[28] G. Karczewski, S. Maćkowski, M. Kutrowski, T. Wojtowicz, and J. Kossut, Appl. Phys. Lett. **74**, 3011 (1999).

[29] Y. Hinuma, A. Grüneis, G. Kresse, and F. Oba, Phys. Rev. B - Condens. Matter Mater. Phys. **90**, 155405 (2014).

[30] D. Mourad, J.-P. Richters, L. Gérard, R. André, J. Bleuse, and H. Mariette, Phys. Rev. B - Condens. Matter Mater. Phys. **86**, 195308 (2012).

[31] S. Raymond, S. Fafard, P. Poole, A. Wojs, P. Hawrylak, S. Charbonneau, D. Leonard, R. Leon, P. Petroff, and J. Merz, Phys. Rev. B - Condens. Matter Mater. Phys. **54**, 11548 (1996).

[32] T. Smoleński, T. Kazimierczuk, M. Goryca, P. Kossacki, J.A. Gaj, P. Wojnar, K. Fronc, M.

Korkusiński, and P. Hawrylak, in *Acta Phys. Pol. A* (Polish Academy of Sciences, 2011), pp. 615–617.

[33] M. Syperek, J. Misiewicz, C.H. Chan, D.O. Dumcenco, Y.S. Huang, and W.C. Chou, Acta Phys. Pol. A **124**, 821 (2013).

[34] U. Hakanson, J. Persson, F. Persson, H. Svensson, L. Montelius, and M.K.-J. Johansson, Nanotechnology **14**, 675 (2003).

[35] T. Kazimierczuk, T. Smoleński, M. Goryca, Kłopotowski, P. Wojnar, K. Fronc, A. Golnik, M. Nawrocki, J.A. Gaj, and P. Kossacki, Phys. Rev. B - Condens. Matter Mater. Phys. **84**, 165319 (2011).

[36] G. Hönig, G. Callsen, A. Schliwa, S. Kalinowski, C. Kindel, S. Kako, Y. Arakawa, D. Bimberg, and A. Hoffmann, Nat. Commun. **5**, 1 (2014).

[37] A. Piryatinski, S.A. Ivanov, S. Tretiak, and V.I. Klimov, Nano Lett. **7**, 108 (2007).

[38] E. Vanelle, A. Alexandrou, and J.P. Likforman, Phys. Rev. B - Condens. Matter Mater. Phys. **53**, R16172 (1996).

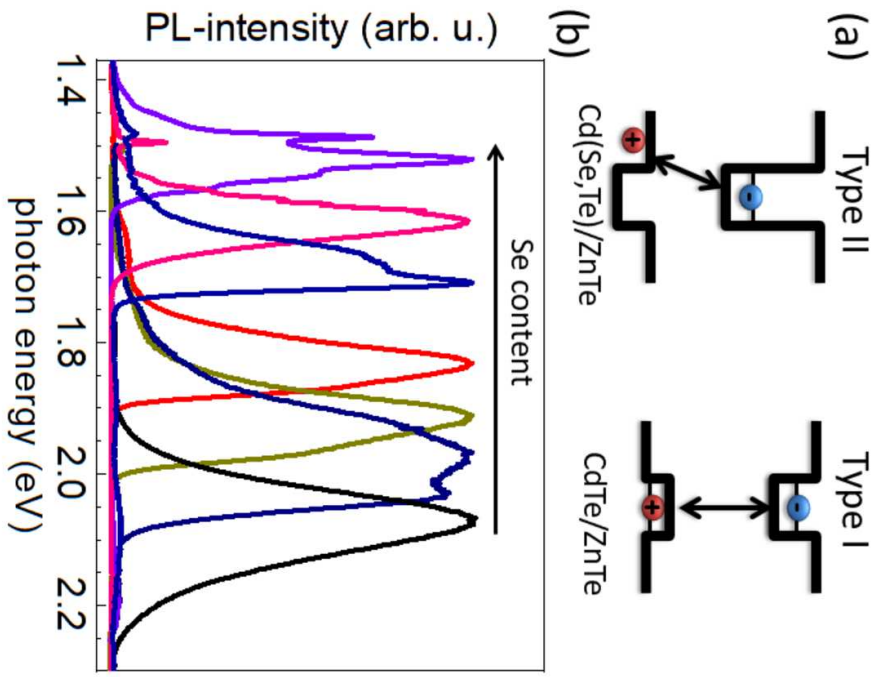

PLEASE CITE THIS ARTICLE AS DOI: 10.1063/5.0016326